TABLE I
COMPARISON OF THE NUMBER OF UNKNOWNS BETWEEN SIE'S AND VIE'S

	SIE	VIE
Square cylinder with N samples on each side	8N	N^2
Cube with N samples on each side	$24N^2$	$3N^3$

graphic data, and by extrapolating bulk dosimetry trends through analysis of many models and parameters similar to the aforementioned one, it is believed that this analysis should constitute a useful diagnostic tool for predicting microwave hazards.

IV. Concluding Remarks

In this short paper the feasibility of using the SIE technique to analyze the fields in arbitrarily shaped lossy dielectric cylinders with a TM or TE incident plane wave has been demonstrated. Generally, this method also applies for any arbitrarily shaped penetrable cylinders composed of both dielectric and magnetic material. Although the illuminating sources considered here are TM and TE plane waves, for near zone sources such as direct contacted aperture sources, corner reflectors, etc., this technique still applies. For dielectric circular cylinders, good agreement is obtained between the SIE solutions and the eigenfunction expansion solutions. For a cylinder with arbitrary cross section, however, the integral equation method, including both the SIE method of this short paper and the volume integral equation (VIE) technique advocated in [6], [11], proves to be definitely more advantageous.

A further breakdown of the comparable computer storage requirement of the two integral equation methods is now in order, since this dictates the maximum sampling rate and hence body size which may be tractable. For conceptual simplicity consider the homogeneous square cylinder and cube. Table I shows the relative number of unknowns, and thus the matrix size, needed for each [16]. To assure that meaningful results are obtained, i.e., sufficient sampling to accurately describe field variations, N should be large. Thus the SIE can be seen to hold a definite advantage (for $N > 8$). It should also be noted that the same sampling rate is assumed for the VIE throughout the interior. In cases where ε_r or σ are large, and wavelength becomes contracted inside the body, a much larger number of samples than that assumed here may actually be needed. If the body is not homogeneous, however, i.e., many layered or even with continuously varying ε and σ, then the VIE approach should prove to be more suitable.

In order to aid in the determination of applicability, the major advantages of each method are summarized here.

VIE Technique:

1) Applicable for arbitrary geometric configurations.
2) Avoids convergence problem of the eigenfunction series.
3) Useful for inhomogeneous bodies.

SIE Technique:

1) Less unknowns are required for homogeneous bodies.
2) Applicable for arbitrary geometric configurations.
3) Avoids convergence problem of the eigenfunction series.

Eigenfunction Expansion Technique:

1) Does not require the storage and inversion of a large matrix.
2) Requires much less computer time.

In conclusion, the problem of predicting fields in arbitrary cylinders of biological tissue has been successfully treated. By the good agreement obtained and useful field contours found, one may conclude that the numerical techniques employed here are advantageous tools. This solution method has also been successfully applied to three-dimensional bodies of revolution [18] and will be presented in a later paper.

Acknowledgment

The authors wish to thank Dr. D. R. Wilton for his many suggestions during the course of this work.

References

[1] W. W. Mumford, "Introductory remarks," *IEEE Trans. Microwave Theory Tech. (Special Issue on Biological Effects of Microwaves)*, vol. MTT-19, p. 130, Feb. 1971.
[2] A. R. Shipiro, R. F. Lutomirski, and H. T. Yura, "Induced fields and heating within a cranial structure irradiated by an electromagnetic plane wave," *IEEE Trans. Microwave Theory Tech.*, vol. MTT-19, pp. 187–196, Feb. 1971.
[3] H. S. Ho, A. W. Guy, R. A. Sigelmann, and J. F. Lehmann, "Microwave heating of simulated human limbs by aperture sources," *IEEE Trans. Microwave Theory Tech.*, vol. MTT-19, pp. 224–231, Feb. 1971.
[4] A. W. Guy, "Analyses of electromagnetic fields induced in biological tissues by thermographic studies on equivalent phantom models," *IEEE Trans. Microwave Theory Tech.*, vol. MTT-19, pp. 205–214, Feb. 1971.
[5] T. C. Tong, "Scattering by a dielectric rectangular cylinder," presented at the 1973 IEEE G-AP Symposium, Boulder, CO, Aug. 1973.
[6] D. E. Livesay and K. M. Chen, "Electromagnetic fields induced inside arbitrarily shaped biological bodies," *IEEE Trans. Microwave Theory Tech.*, vol. MTT-22, pp. 1273–1280, Dec. 1974.
[7] J. A. Stratton, *Electromagnetic Theory*. New York: McGraw-Hill, ch. 3, 1941.
[8] A. J. Poggio and E. K. Miller, "Integral equation solutions of three-dimensional scattering problems," *Computer Techniques for Electromagnetics*, R. Mittra Ed., Pergamon Press, 1973.
[9] R. F. Harrington, *Field Computation by Moment Methods*. New York: McGraw-Hill, pp. 230–238, 261, 1961.
[10] R. F. Harrington, *Time Harmonic Electromagnetic Fields*. New York: McGraw-Hill, 1961.
[11] J. H. Richmond, "Scattering by a dielectric cylinder of arbitrary cross section shape," *IEEE Trans. Antennas Propagat.*, vol. AP-13, p. 334, May 1965.
[12] T. K. Wu and L. L. Tsai, "Shielding properties of thick conducting cylindrical shells," *IEEE Trans. Electromag. Compat.*, vol. EMC-16, pp. 201–204. Nov. 1974.
[13] M. Abramowitz and T. Stegun, *Handbook of Mathematical Functions*, NBS AMS-55.
[14] J. E. Lewis, T. K. Sarkar, and P. D. O'Kelly, "Generation of Bessel functions of complex order and argument," *Electron. Lett.*, vol. 7, pp. 615–616, Oct. 1971.
[15] T. K. Wu and L. L. Tsai, "Numerical analysis of electromagnetic fields in biological tissues," *IEEE Proc.*, vol. 62, pp. 1167–1168, Aug. 1974.
[16] T. K. Wu, "Electromagnetic scattering from arbitrarily-shaped lossy dielectric bodies," Ph.D. dissertation, University of Mississippi, University, 1976.
[17] Yu Chang and R. F. Harrington, "A surface formulation for characteristic modes of material bodies," Syracuse University, Electrical and Computer Engineering Dept. Tech. Report, No. 2, Contract N000A-67-A-0378-006, 1976.
[18] L. L. Tsai and T. K. Wu, "Scattering from lossy dielectric bodies of revolution," *1975 USNC/URSI Meeting Digest*, Boulder, CO, p. 128, Oct. 1975.
[19] J. R. Wait, *Electromagnetic Radiation from Cylindrical Structures*. New York: Pergamon Press, 1959.
[20] C. C. Johnson, C. H. Durney, and H. Massoudi, "Long-wavelength electromagnetic power absorption in prolate spheroidal models of man and animals," *IEEE Trans. Microwave Theory Tech.*, vol. MTT-23, pp. 739–747, Sept. 1975.

Field and Power Density Distributions of the Dipolar Modes in a Partially Filled Cylindrical Plasma Waveguide

GAR LAM YIP, SENIOR MEMBER, IEEE, AND SON LE-NGOC

***Abstract*—The field and power density distributions for the dipolar modes in a partially filled plasma waveguide have been studied at operating points in the vicinity of the plasma, the surface wave, and the gyro**

Manuscript received June 30, 1975; revised April 30, 1976. This work was supported by the National Research Council of Canada.
G. L. Yip is with the Department of Electrical Engineering, McGill University, Montreal, P.Q., Canada.
S. Le-Ngoc was with the Department of Electrical Engineering, McGill University, Montreal, P.Q., Canada. He is now with Pratt and Whitney Aircraft, Montreal, P.Q., Canada.

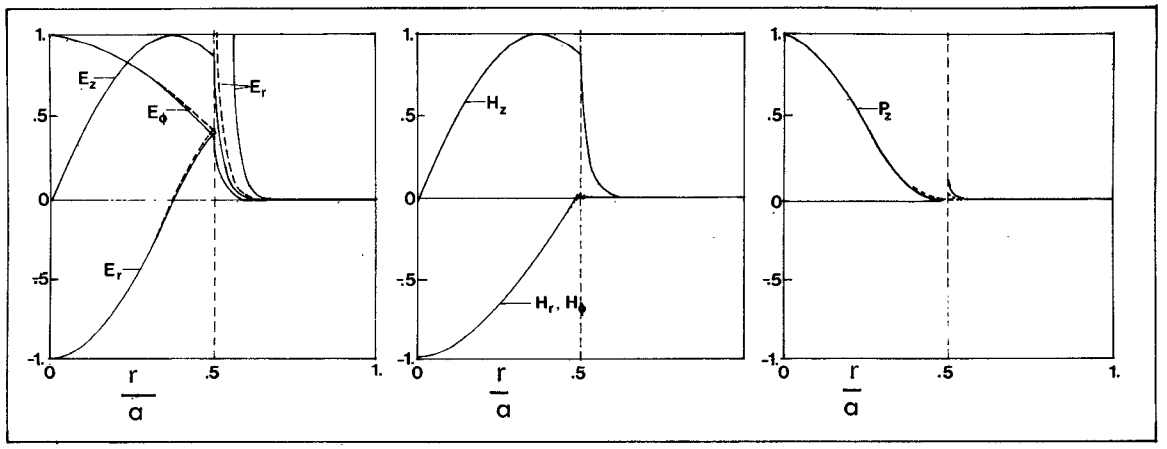

Fig. 1. Radial field and power density distributions near the gyro resonance. (a) $^{0.5}P^{0.5}_{1,1}$, $\Omega = 0.495$, $\Omega\beta\gamma = 40.842$ (39.635), $|E_z(\max)| = 0.581$ (0.581, $|E_r(\max)| = 0.636 \times 10^{-1}$(0.617 $\times$ 10^{-1}), $|E_\phi(\max)| = 0.636 \times 10^{-1}$(0.617 $\times$ 10^{-1}), $|H_z(\max)| = 0.215 \times 10^{-1}$, $|H_r(\max)| = 0.310$ (0.312), $|H_\phi(\max)| = 0.310$ (0.312), $|P_z(\max)| = 0.197 \times 10^{-1}$ (0.192 $\times$ 10^{-1}). (b) $^{0.5}P^{0.5}_{1,1}$, $\Omega = 0.495$, $\Omega\beta\gamma = 84.395$ (83.813), $|E_z(\max)| = 0.580$ (0.580), $|E_r(\max)| = 0.610 \times 10^{-1}$ (0.615 $\times$ 10^{-1}), $|E_\phi(\max)| = 0.612 \times 10^{-1}$(0.616 $\times$ 10^{-1}), $|H_z(\max)| = 0.103 \times 10^{-1}$, $|H_r(\max)| = 0.710 \times 10^{-1}$(0.719 $\times$ 10^{-1}), $|H_\phi(\max)| = 0.715 \times 10^{-1}$(0.717 $\times$ 10^{-1}), $|P_z(\max)| = 0.215 \times 10^{-2}$(0.215 $\times$ 10^{-2}).

resonant frequencies. Results of both the quasi-static and exact analyses are presented. From the field distributions, the behavior of electrons at each resonance is clearly explained.

I. Introduction

The dispersion characteristics of the dipolar modes in a partially filled plasma waveguide have been extensively studied in an earlier paper [1]. The purpose of the present short paper is to extend our work by examining the radial field distributions, especially near the resonant frequencies.

The normalized parameters which characterize the plasma are $\Omega = \omega/\omega_p$ and $R = \omega_c/\omega_p$, where ω, ω_p, and ω_c are the angular wave, the plasma, and the gyro frequencies, respectively. The normalized waveguide radius is denoted by $\beta = \omega_p(a/c)$, where a is the waveguide radius and c is the velocity of light in free space. The variation with the axial and azimuthal positions and time is of the form $\exp\{j(kz + n\phi - \omega t)\}$, where k is the axial propagation constant and $n = \pm 1$ for dipolar modes. The normalized propagation constant is $\gamma = k/k_0$, where k_0 is the propagation constant in free space. The radial propagation constants in the plasma region are denoted by U_1 and U_2 in the exact analysis and U is the electrostatic approximation, while that in free space is denoted by U_0. As before [1], the plasma has been assumed collisionless.

The exact field solutions can be derived directly from the Maxwell's equations through the usual techniques [1]–[3]. In the electrostatic approximation, the ac magnetic field is first neglected, and the electric field is derived from a scalar potential [4]. However, to obtain the power density for the case at hand, it is necessary to approximate the ac magnetic field from the Maxwell's equation, $\nabla \times \boldsymbol{H} = -jk_0\bar{\bar{\varepsilon}} \cdot \boldsymbol{E}$. Subject to the boundary condition, it can be shown that the longitudinal component of the ac magnetic field can always be zero. Hence the field solutions lead to purely transverse magnetic (TM) modes. In the exact analysis, it can be shown analytically that the field solutions are also TM modes when γ tends to infinity.

It is noted that the field and power density distributions plotted are normalized with respect to their maximum magnitude inside the plasma region, i.e., $0 \leq r/a \leq 0.5$, which is also indicated for reference. The results of the electrostatic approximation are written inside a bracket beside the exact results. For comparison, both results are presented in the same figure with the solid and the broken lines for the exact and electrostatic analysis, respectively.

II. Numerical Results and Discussions

For the sake of brevity, the detailed expressions for the field components E_r, E_ϕ, and E_z inside and outside the plasma region

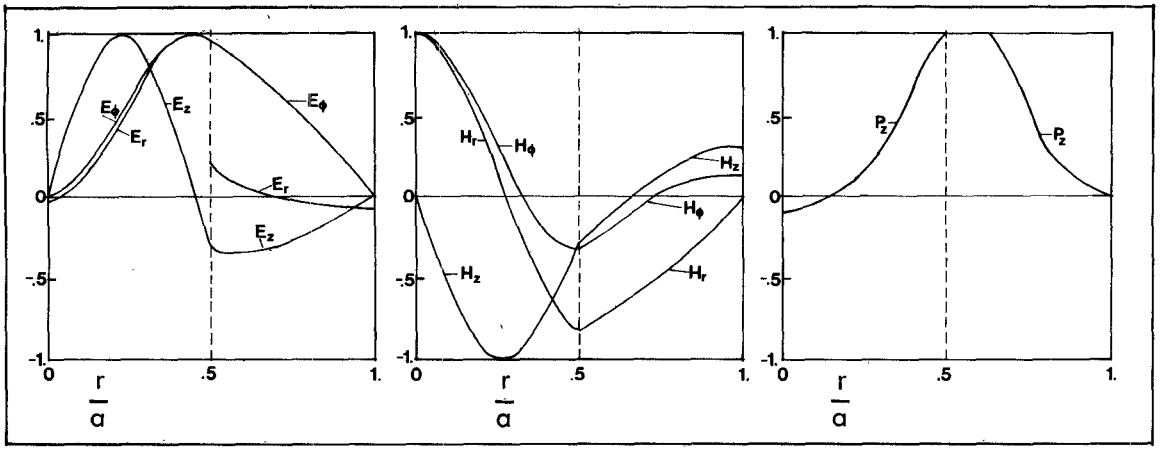

(a)

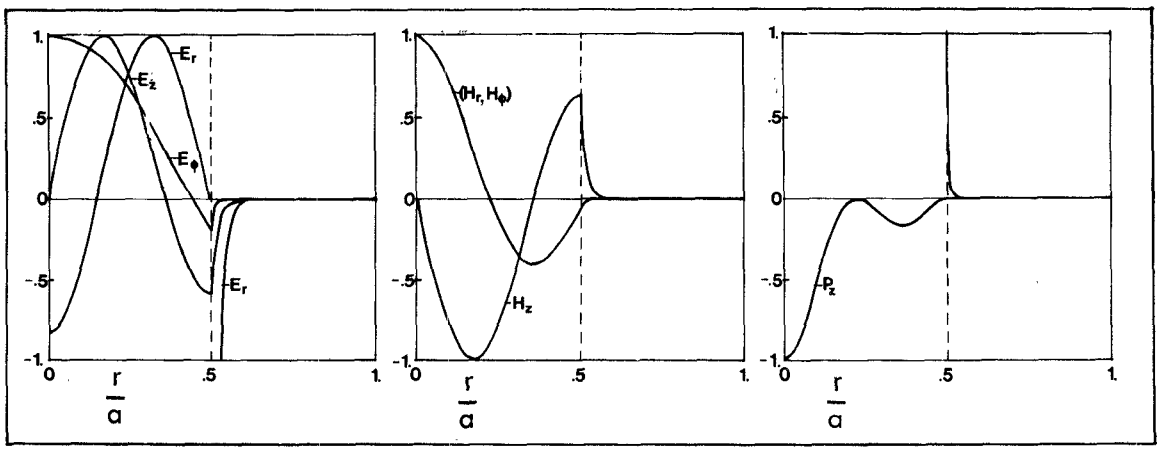

(b)

Fig. 2. Radial field and power density distributions near the gyro resonant frequency. (a) ${}^{5}_{1}C^{0.5}_{1,1}$, $\Omega = 5.002$, $\Omega\beta\gamma = 2.273145$, $|E_z(\max)| = 0.3740$, $|E_r(\max)| = 0.846$, $|E_\phi(\max)| = 0.8348$, $|H_z(\max)| = 1.367$, $|H_r(\max)| = 0.4984$, $|H_\phi(\max)| = 0.4985$, $|P_z(\max)| = 0.9622 \times 10^{-1}$. (b) ${}^{0.5}_{1}C^{0.5}_{-1,1}$, $\Omega = 5.002$, $\Omega\beta\gamma = 57.63752$, $|E_z(\max)| = 0.5811$,$|E_r(\max)| = 0.6261 \times 10^{-1}$, $|E_\phi(\max)| = 0.5332 \times 10^{-1}$, $|H_z(\max)| = 0.485 \times 10^{-1}$, $|H_r(\max)| = 0.4494$, $|H_\phi(\max)| = 0.4494$, $|P_z(\max)| = 0.2391 \times 10^{-1}$.

in both the electrostatic and exact analyses are not given here, but can be found in [5, ch. 3, 4].

Fig. 1(a) and (b) represents the field and power density distributions at an operating point on the dispersion curves for the plasma modes ${}^{0.5}_{1}P^{0.5}_{1,1}$ and ${}^{0.5}_{1}P^{0.5}_{-1,1}$, respectively. In the notation ${}^{R}_{\beta}P^{S_0}_{n,m}$, P represents the plasma modes, R,β,n are as defined before, $S_0 = b/a$ is the ratio of the plasma column and waveguide radii, and m is the mode order. This operating point is in the gyro resonance region and near the gyro resonant frequency. The agreement between the two results is observed except for E_r and P_z in the free-space region. Since H_z is very small compared with the other components, hence the prediction that H_z vanishes in the electrostatic approximation is verified. The waves are therefore transverse magnetic. On the axis of the plasma column, the transverse components of the electric field demonstrate the right-hand, i.e., $E_r = -jE_\phi$, and the left-hand, i.e., $E_r = +jE_\phi$ circular polarization for $n = 1$ and $n = -1$, respectively. The circularly polarized nature of the waves increases as Ω tends to R. However, the operating points used by Bevc [2] are not near the resonant frequencies, i.e., γ is small. The circularly polarized waves cause the electrons to gyrate about the dc magnetic field line. The power density is positive, so the power flows in the same direction of wave propagation. Hence the wave is forward. The maximum magnitude of P_z is so small that the power flow can be considered as almost vanishing. The energy carried by the waves is transferred to the kinetic energy of the electrons, resulting in the maximum gyration of the electrons at the gyro resonance frequency $\Omega_\infty = R$.

To see the circularly polarized nature of the waves more clearly for small values of γ as Ω approaches R, the field and power distributions for the ${}^{5}_{1}C^{0.5}_{1,1}$ (C stands for cyclotron modes) at $\Omega = 5.002$, $\Omega\beta\gamma = 2.273145$ [1, fig. 6(c)] are presented in Fig. 2(a), where $|E_r| \simeq |E_\phi|$ in the plasma region. Since the operating point is far away from the resonance condition ($\gamma \to \infty$), there is an appreciable amount of positive power carried in the circularly polarized waves, showing the forward nature of the waves. As the resonance condition is approached, e.g., $\gamma\beta\Omega = 57.63752$ as in Fig. 2(b), it is seen that power flow becomes extremely small, and the electric field exhibits circular polarization only on the axis because by now most of the wave energy has been converted into the gyrations of the electrons. The group velocity approaches zero [1, fig. 6(c)]. Nevertheless, the magnetic field still exhibits circular polarization inside the plasma. All the aforementioned observations have been checked analytically, using the field expressions given earlier.

Fig. 3(a) and (b) represents the field and power density distributions at an operating point on the dispersion curves for the cyclotron modes, ${}^{0.5}_{1}C^{0.5}_{1,1}$ and ${}^{0.5}_{1}C^{0.5}_{-1,1}$, respectively. The agreement between the two results is still observed for the electric field and the power density. It is obvious that the magnetic

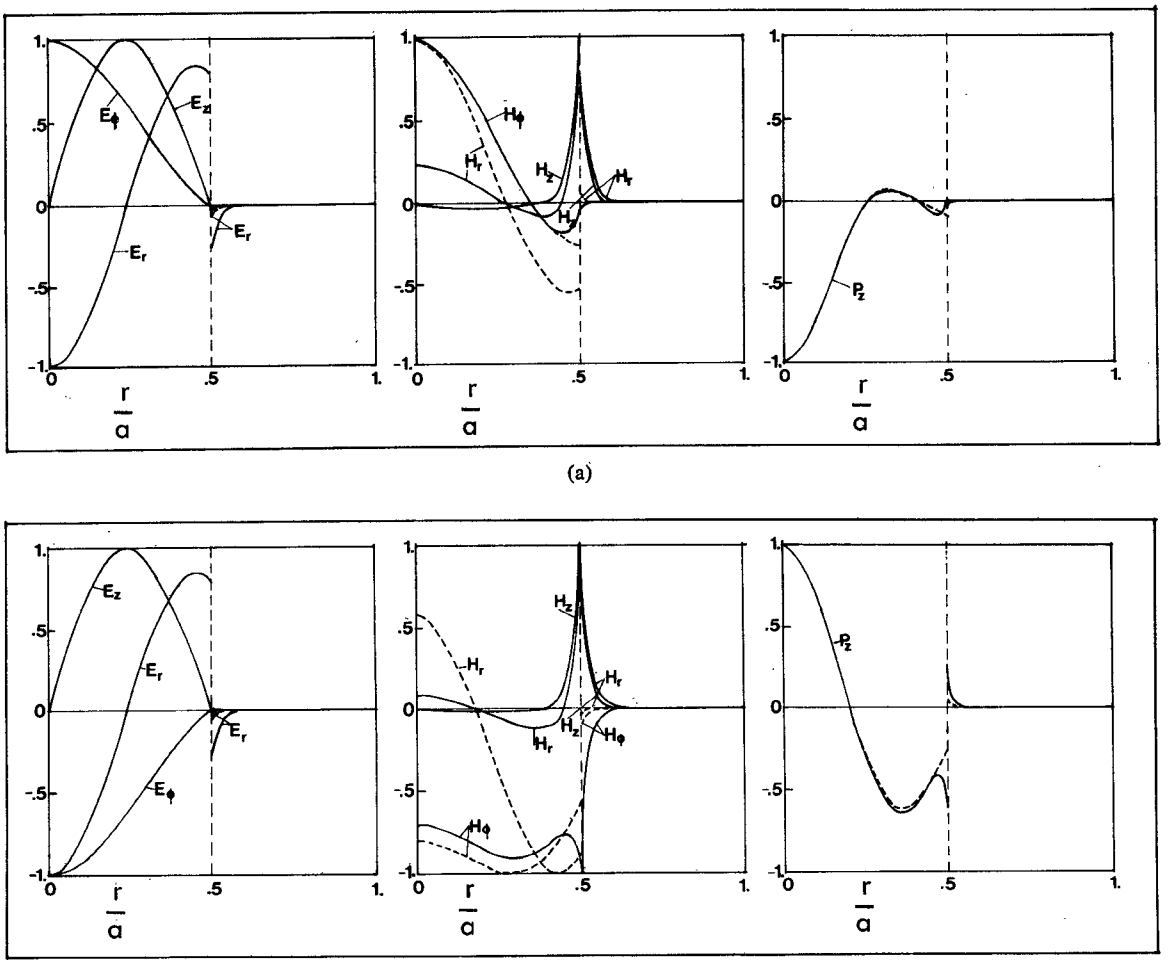

Fig. 3. Radial field and power density distributions near the plasma resonance. (a) ${}^{5}_{1}C^{0.5}_{1}$, $\Omega = 1.005$, $\Omega\beta\gamma = 43.833$ (43.853), $|E_z(\max)| = 0.581$ (0.581), $|E_r(\max)| = 0.884 \times 10^{-1}$ (0.881×10^{-1}), $|E_\phi(\max) = 0.885 \times 10^{-1}$($0.885 \times 10^{-1}$), $|H_z(\max)| = 0.949 \times 10^{-2}$, $|H_r(\max)| = 0.825 \times 10^{-2}$($0.196 \times 10^{-2}$), $|H_\phi(\max)| = 0.193 \times 10^{-2}$($0.196 \times 10^{-2}$), $|P_z(\max)| = 0.171 \times 10^{-3}$($0.174 \times 10^{-3}$). (b) ${}^{0.5}_{1}C^{0.5}_{1,1}$, $\Omega = 1.005$, $\Omega\beta\gamma = 43.798$ (43.817), $|Ez(\max)| = 0.581$ (0.581), $|E_r(\max)| = 0.885 \times 10^{-1}$. ($0.884 \times 10^{-1}$), $|E_\phi(\max)| = 0.886 \times 10^{-1}$ (0.885×10^{-1}), $|H_z(\max)| = 0.924 \times 10^{-2}$, $|H_r(\max)| = 0.801 \times 10^{-2}$ (0.117×10^{-2}), $|H_\phi(\max)| = 0.921 \times 10^{-3}$ (0.854×10^{-3}), $|P_z(\max)| = 0.571 \times 10^{-4}$ (0.608×10^{-4}).

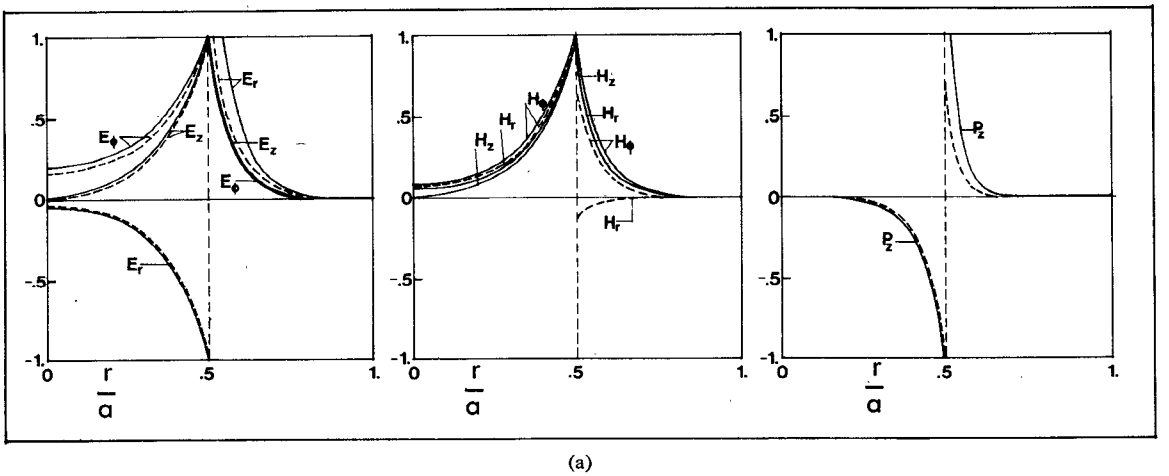

Fig. 4. Radial field and power density distributions near the surface-wave resonance. (a) ${}^{0.5}_{1}S^{0.5}_{0}$ $\Omega = 0.8, \Omega\beta\gamma = 13.642$ (14.687), $|E_z(\max)| = 0.109 \times 10^{2}$ (0.141×10^{2}), $|E_r(\max)| = 0.594 \times 10^{1}$ (0.771×10^{1}), $|E_\phi(\max)| = 0.152 \times 10^{1}$ (0.192×10^{1}), $|H_z(\max)| = 0.798$, $|H_r(\max)| = 0.122 \times 10^{1}$ (0.837), $|H_\phi(\max)| = 0.806$ (0.824), $|P_z(\max)| = 0.333 \times 10^{1}$ (0.398×10^{1}). (b) ${}^{0.5}_{1}S^{0.5}_{1}$, $\Omega = 0.77$, $\Omega\beta\gamma = 45.078$ (45.012), $|E_z(\max)| = 0.770 \times 10^{5}$ (0.748×10^{5}), $|E_r(\max)| = 0.445 \times 10^{5}$ (0.432×10^{5}), $|E_\phi(\max) = 0.346 \times 10^{5}$ (0.332×10^{5}), $|H_z(\max)| = 0.175 \times 10^{5}$, $|H_r(\max)| = 0.250 \times 10^{5}$ (0.129×10^{5}), $|H_\phi(\max)| = 0.125 \times 10^{4}$ (0.131×10^{4}), $|P_z(\max)| = 0.239 \times 10^{8}$ (0.262×10^{8}). Radial field and power density distributions near the gyro resonance. (c) ${}^{0.5}_{1}S^{0.5}_{1}$, $\Omega = 1.505$, $\Omega\beta\gamma = 44.994$ (48.467), $|E_z(\max)| = 0.581$ (0.581), $|E_r(\max)| = 0.430 \times 10^{-1}$ (0.461×10^{-1}), $|E_\phi(\max)| = 0.431 \times 10^{-1}$ (0.461×10^{-1}), $|H_z(\max)| = 0.109 \times 10^{-1}$, $|H_r(\max)| = 0.189$ (0.188,) $|H_\phi(\max)| = 0.189$ (0.188), $|P_z(\max)| = 0.815 \times 10^{-2}$ (0.871×10^{-2}). Radial field and power density distributions near the plasma resonance. (d) ${}^{0.5}_{1}S^{0.5}_{1}$, $\Omega = 0.99$, $\Omega\beta\gamma = 68.554$ (68.201), $|E_z(\max)| = 0.581$), $|E_r(\max)| = 0.531 \times 10^{-1}$ (0.531×10^{-1}), $|E_\phi(\max)| = 0.532 \times 10^{-1}$ (0.532×10^{-1}), $|H_z(\max)| = 0.609 \times 10^{-1}$, $|H_r(\max)| = 0.593 \times 10^{-1}$ (0.101×10^{-2}), $|H_\phi(\max)| = 0.296 \times 10^{-2}$ (0.126×10^{-2}), $|P_z(\max)| = 0.295 \times 10^{-4}$ (0.312×10^{-4}).

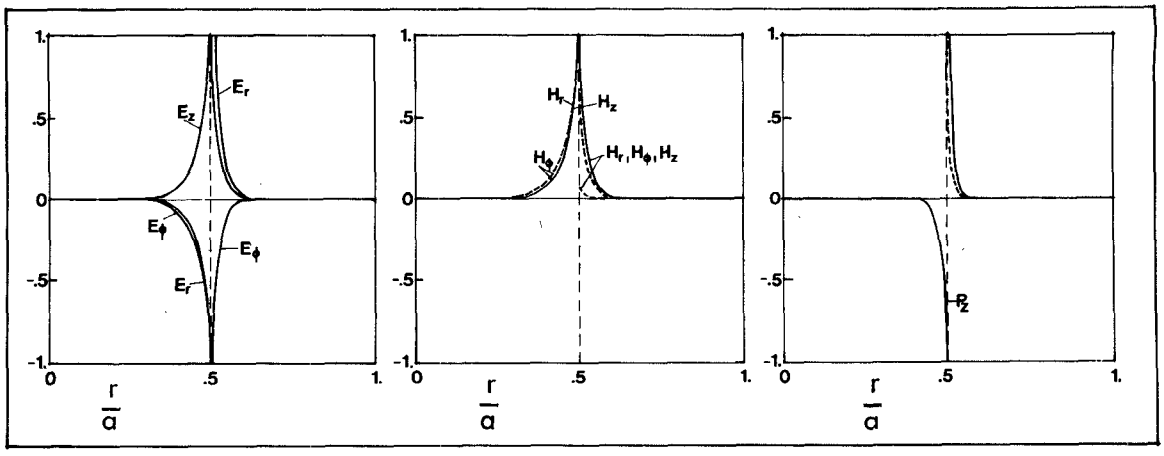

(b)

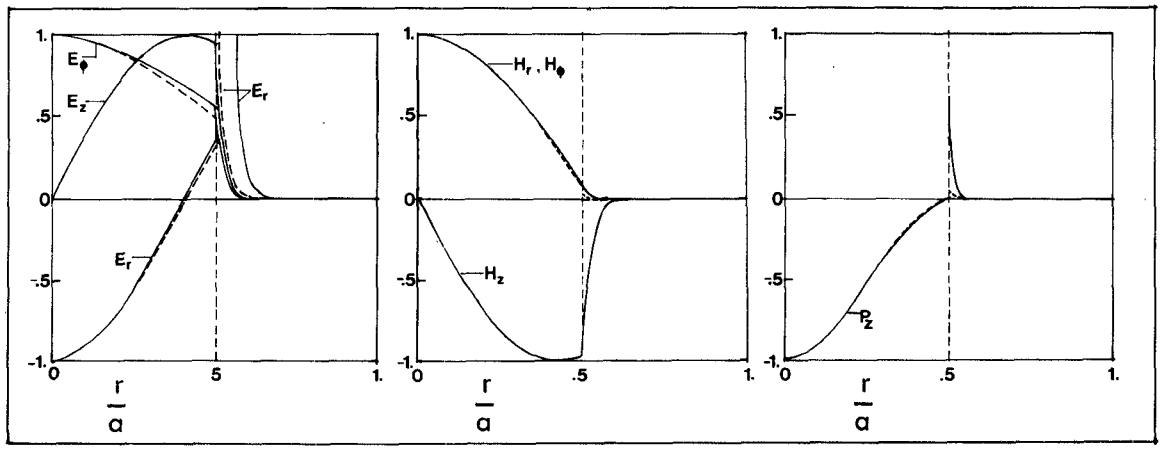

(c)

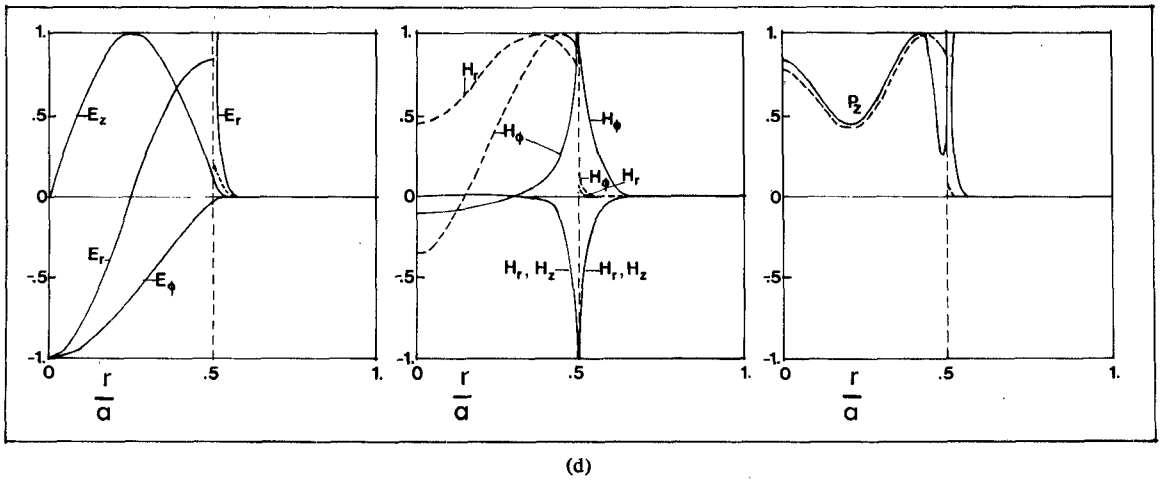

(d)

Fig. 4 (*Continued*).

fields are so small that they can be neglected with respect to the electric fields. This fact is also verified analytically. The fields are therefore electrostatic as assumed in the electrostatic approximation. The longitudinal component of the electric field is much stronger than the other ones. This field is associated with the electron oscillation along the dc magnetic field lines. The maximum magnitude of P_z is again so small that power flow can be considered as vanishing. The energy carried by the waves is transferred to the kinetic energy of electrons to support their longitudinal oscillations at the plasma resonance frequency $\Omega_\infty = 1$. The total power flow is negative. Hence the wave is backward.

Fig. 4(a) and (b) represents the field and power density distributions at an operating point on the dispersion curves for the surface-wave modes ${}^{0.5}_{1.}S^{0.5}_{1}$ and ${}^{0.5}_{1.}S^{0.5}_{-1}$, respectively. This operating point is in the surface-wave region, i.e., U_1, U_2, and U are imaginary, and near the surface-wave resonance frequency. It can be seen that the agreement of the two results is better in Fig. 4(b) where $n = -1$ than in Fig. 4(a) where $n = 1$. This fact has also been observed in the dispersion characteristics [1]. In both figures the field components have their highest values at the plasma–air interface and decrease rapidly from the interface. This field behavior is characteristic of surface waves. The transverse electric field excites the transverse oscillation of the electrons.

The power density also has the highest values at the interface. So the energy carried by the wave is concentrated near the interface. This wave is therefore called the surface wave. The power densities inside and outside the plasma column are in opposite directions. The areas under these curves add to almost zero, leading to the conclusion that the total power flow also vanishes. The wave energy is transferred to the kinetic energy of the electrons to support the transverse oscillation of the electrons at the surface-wave resonance frequency $\Omega_\infty = (\Omega_U/\sqrt{2})$.

Fig. 4(c) and (d) respresents the field and power density distributions at an operating point on the dispersion curves for the surface-wave modes ${}^{1.5}_{1.}S^{0.5}_{1}$ and ${}^{1.5}_{1.}S^{0.5}_{-1}$. As pointed out previously [1], these surface-wave modes undergo some fundamental change. The operating point on ${}^{1.5}_{1.}S^{0.5}_{1}$ and that on ${}^{1.5}_{1.}S^{0.5}_{-1}$ are near the cyclotron and the plasma resonance frequencies, respectively. In Fig. 4(c) similar results are obtained for the electric fields as discussed previously in Fig. 1(a). However, the magnetic fields are seen to be in opposite directions. The total power flow is negative. Hence the wave is backward. The same results are also seen for the field and power density distributions at an operating point on the dispersion curves for the cyclotron modes, ${}^{1.5}_{1.}C^{0.5}_{\pm 1,1}$, so these results are not presented here. In Fig. 4(d) the agreement of the two results is only seen in the electric field and power density. The discrepancies in the magnetic fields are clearly observed. However, they do not cause any severe error in the overall results because the magnitudes of the magnetic fields are so small that they can be neglected with respect to the electric field. The power density is positive, so the wave is forward. Similar results are also seen of the field and power density distributions for the plasma modes, ${}^{1.5}_{1.}P^{0.5}_{\pm 1,1}$, so these results are not presented here.

In all the figures it is clear that E_r is always discontinuous at the plasma–air interface. This can be explained by the fact that a surface-charge layer exists on the interface due to the different mobilities of ions and electrons [3]. In the electrostatic results, it is seen that H_r, H_ϕ are usually discontinuous because they have not been subjected to the boundary conditions, but are only approximated by using the Maxwell's equation as indicated previously. However, the results obtained for the power density still agree with the exact ones.

III. Conclusions

From the preceding discussion, it can be summarized that near the plasma resonance frequency the fields are static. However, near the cyclotron and the surface-wave frequency, the waves are characterized by TM modes, i.e., $H_z \simeq 0$, in which the transverse components are much stronger. As R increases beyond 1, the surface waves, i.e., ${}^{R}_{\beta}S^{s_0}_{n}$, undergo some fundamental change. They become bulk waves for large γ. Near the plasma resonance, the ${}^{R}_{\beta}S^{s_0}_{-1}$ waves behave like the plasma modes. Near the cyclotron resonance, the ${}^{R}_{\beta}S^{s_0}_{1}$ waves behave like the cyclotron modes. This latter aspect has been discussed previously in connection with the dispersion characteristics [1].

The results obtained by assuming collisionless plasma are also valid for the cold plasma used in the laboratory because plasma and surface-wave modes have already been verified in the laboratory by several investigators [6]–[8].

References

[1] G. L. Yip and S. Le-Ngoc, "Dispersion characteristics of the dipolar modes in a waveguide partially-filled with a magnetoplasma column," *Can. J. Phys.*, vol. 53, pp. 1163–1178, June 1975.
[2] V. Bevc, "Surface and bulk waves on axially magnetized plasma column," *J. Appl. Phys.*, vol. 40, pp. 633–640, Feb. 1969.
[3] R. Likuski, "Free and driven modes in anisotropic plasma guides and resonators," Tech. Documentary Rept. AL-TOR-64-157, Dept. of Elect. Engineering, Univ. of Illinois, July 1964.
[4] A. W. Trivelpiece and R. W. Gould, "Space charge waves in cylindrical plasma columns," *J. Appl. Phys.*, vol. 30, pp. 1784–1793, Nov. 1959
[5] S. Le-Ngoc, "Electromagnetic wave propagation in partially-filled anisotropic waveguides," Doctoral dissertation, Dept. of Electrical Engineering, McGill University, Aug. 1975.
[6] A. W. Trivelpiece, "Slow-wave propagation in plasma waveguides," Tech. Report No. 7, California Institute of Technology, 1957.
[7] R. N. Carlile, "A backward-wave surface mode in a plasma waveguide," *J. Appl. Phys.*, vol. 35, pp. 1384, 1964.
[8] H. L. Stover and G. S. Kino, "A field theory for propagation along a non-uniform plasma," *Proc. 5th Int. Congress on Microwave Tables*, Paris, France, p. 374, 1964.